DNA Nanotechnology

DOI: 10.1002/anie.201404307

Synchronization of Two Assembly Processes To Build Responsive DNA Nanostructures**

Zhou Nie, Pengfei Wang, Cheng Tian, and Chengde Mao**

Abstract: *Herein, we report a strategy for the synchronization of two self-assembly processes to assemble stimulus-responsive DNA nanostructures under isothermal conditions. We hypothesized that two independent assembly processes, when brought into proximity in space, could be synchronized and would exhibit positive synergy. To demonstrate this strategy, we assembled a ladderlike DNA nanostructure and a ringlike DNA nanostructure through two hybridization chain reactions (HCRs) and an HCR in combination with T-junction cohesion, respectively. Such proximity-induced synchronization adds a new element to the tool box of DNA nanotechnology. We believe that it will be a useful approach for the assembly of complex and responsive nanostructures.*

DNA is a promising building block for controllable self-assembly because of its sequence-specific base pairing and well-established double-helix structure.[1] A temperature or denaturant gradient is commonly used to promote desired DNA hybridization and facilitates the formation of thermodynamically stable DNA nanostructures.[2] Such an approach is different from in vivo molecular self-assembly, which is often tightly regulated under isothermal conditions. For example, the assembly of actin filaments can be triggered by receptor-mediated signal transduction.[3] The question of how to mimic such delicate biological self-assembly is not only intellectually challenging, but the ability to do so would also be useful for the development of dynamic switches or responsive materials. Some preliminary attempts have been made in this direction for DNA self-assembly.[4] Herein we demonstrate a responsive molecular system in which two DNA-assembly processes could be initiated by an initiator and synchronized to produce complex DNA nanostructures (ladderlike or ringlike structures).

[*] Prof. Dr. Z. Nie
State Key Laboratory of Chemo/Biosensing and Chemometrics
College of Chemistry and Chemical Engineering, Hunan University
Changsha 410082 (P.R. China)
E-mail: niezhou.hnu@gmail.com
C. Tian, Prof. Dr. C. Mao
Department of Chemistry, Purdue University
West Lafayette, IN 47907 (USA)
E-mail: mao@purdue.edu
P. F. Wang
Weldon School of Biomedical Engineering, Purdue University
West Lafayette, IN 47907 (USA)

[**] We thank the NSF and the ONR for supporting this research. Z.N. thanks the China Scholarship Council and the NSFC (No. 21222507) for financial support.

Supporting information for this article is available on the WWW under http://dx.doi.org/10.1002/anie.201404307.

The current research is built on the strand-displacement-based hybridization chain reaction (HCR),[4] an idea originally demonstrated by Dirks and Pierce.[4a] In HCR, an initiator strand hybridizes with one tail-hairpin molecule and opens the hairpin. The opened hairpin can hybridize with another type of tail-hairpin molecule and opens the second hairpin. The hybridization cycle continues between the two types of tail-hairpin strands and eventually produces a long DNA duplex. Although it is an elegant idea, the resulting structures, in most cases, are simple duplexes. We were therefore prompted to ask the question: Can HCR be used to assemble more-complex nanostructures?

The central concept of our strategy is to synchronize multiple assembly processes, either two HCR reactions (for nanoladders, Figure 1 a,b) or one HCR reaction plus one T-junction cohesion (for nanorings, Figure 1 c,d), which are otherwise independent from one another. For the triggered assembly of nanoladders, the system consists of two basic assembly motifs of different types (M1 and M2) and one initiator motif (IL). Each motif is a homodimer. An assembly motif, M1 or M2, contains two identical hairpin strands that are structured into three domains: a central duplex with a length of 1.5 turns and two flanking tail-hairpin structures. Motif IL is a palindromic DNA duplex with a length of 1.5 turns and identical single-stranded tails at each end. The assembly system is organized into two identical HCR cascades (I1–H1–H2) that are physically linked together. When one HCR reaction proceeds, the other will be brought into proximity and will take place at an accelerated speed. Thus, a positive cooperativity is expected. The end products of the synchronized HCR reactions will have a ladderlike structure: two long parallel DNA duplexes are connected by a series of short DNA duplexes (rungs). In the current design, the length of the short duplex (rung) was chosen to be 1.5 turns or 16 base pairs (bps), corresponding to 5.4 nm; the distance between two adjacent rungs is 2.5 turns or 26 bps, corresponding to 8.8 nm. Both distances can be readily resolved by atomic force microscopy (AFM).

The assembly was first analyzed by agarose gel electrophoresis (Figure 2 a). Motifs M1, M2, and IL were separately prepared in TAE/Mg^{2+} buffer, a neutral aqueous buffer containing Mg^{2+}. When motifs M1 and M2 were simply mixed at an equal molar ratio at room temperature (22 °C) in the absence of IL, no assembly occurred, and no species with a high molecular weight (MW) were observed in the gel. Upon the addition of IL (M1/M2/IL = 10:10:1), HCR was initiated, and DNA complexes with high molecular weights appeared as a widely distributed smear in the gel. This process completely depleted the assembly motifs M1 and M2; no corresponding individual motifs were left. This observation

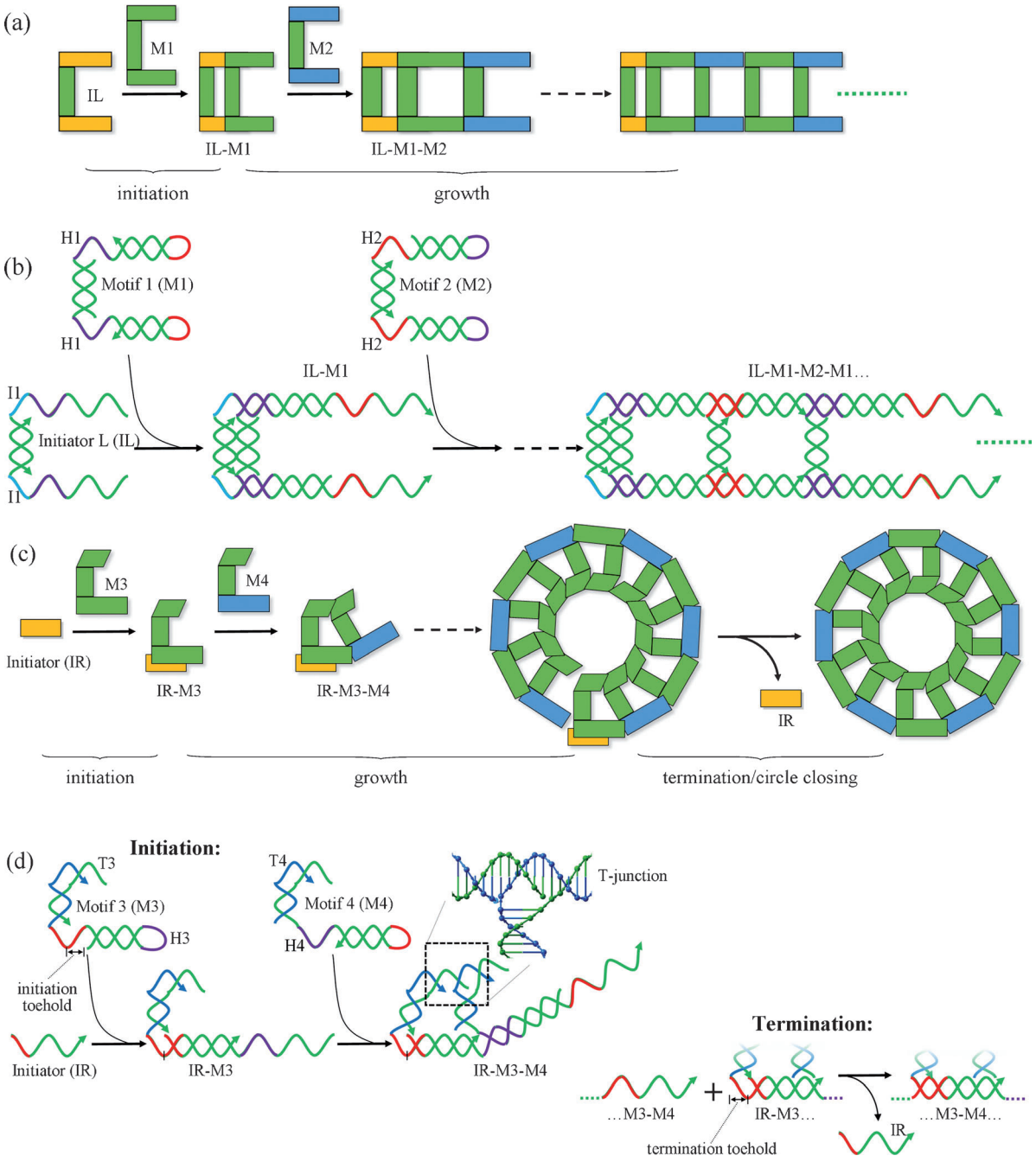

Figure 1. a,c) Simple schematic illustration and b,d) structural details of the synchronized assembly of DNA nanoladders (a,b) and nanorings (c,d) in response to initiators. Motifs IL, M1, and M2 are homodimers of strand I1, H1, and H2, respectively. Motifs M3 and M4 are heterodimers of strands H3 + T3 and H4 + T4, respectively. There are several versions of strand IR, named as IR-*n*, in which *n* corresponds to the length of the red segment (initiation toehold); that is, IR-5 indicates that the red segment is 5 nt long. For any design in (c,d), the sum of the lengths of the initiation toehold and termination toehold is 9 nt, which is identical to the entire length of the toehold of the H3 strand.

was consistent with the formation of designed nanoladders. Interestingly, such nanoladders could not be assembled directly by thermal annealing of the corresponding DNA strands, which only gave DNA complexes with low molecular weights (lane T.A. in Figure 2a). The isothermally assembled DNA nanoladders were further characterized by AFM imaging (Figure 2b–e; see also Figure S1 in the Supporting Information) as linear structures with different lengths randomly distributed on a mica surface. At a higher magnification, ladderlike structures were clearly visible. The observed spacing between adjacent rungs ranged from 9 to 10.8 nm, which closely matched the distances calculated from the model.

The ratio between the concentration of assembly motifs M1 and M2 and that of the initiator IL greatly influenced the assembly. It positively correlated with the molecular weight of the assembled DNA ladder and the polymerization extent. Both electrophoresis (see Figure S2a) and AFM imaging (see

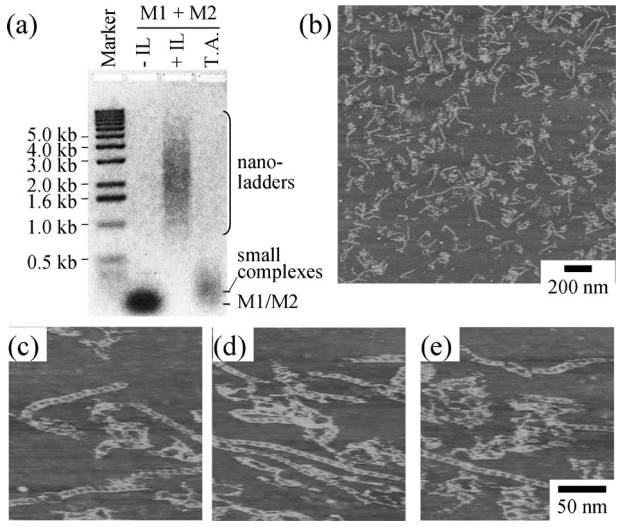

Figure 2. Analysis of the self-assembly of DNA nanoladders. a) Native agarose gel (1.5%) electrophoresis. Sample compositions are indicated above the gel, and the chemical identity of the bands is suggested beside the gel. All component strands of M1 and M2 were directly thermally annealed and used as a control (lane "T.A."). b) Large-area atomic force microscopy (AFM) image of the assembled DNA nanoladders. c–e) Three close-up views of the AFM image. For both electrophoresis and AFM imaging, the DNA concentrations were 500 nM M1, 500 nM M2, and 50 nM IL.

Figure S2 b–d) suggested that the higher the M/IL molar ratio is, the higher the molecular weights of the resulting polymers are. When the M/IL ratio was increased from 5:1 to 10:1, the average length of the DNA ladders increased from about 103 to 129 nm. When the ratio was further increased to 20:1, the average ladder length increased to approximately 182 nm. However, at such a high ratio, the ladders coil into aggregates, presumably because the two tails of DNA ladders released during polymerization or the trigger reacts with two motifs to generate branches in the presence of a large excess of the motifs. Thus, the M/IL ratio influences not only the polymerization extent but also the morphology of the assembled DNA complexes.

To further demonstrate the concept of "synchronization", we applied it to the assembly of DNA nanorings (Figure 1 c,d). In this case, one HCR and one T-junction cohesion[5] are synchronized. The two assembly processes involve different DNA-duplex lengths. This length mismatch forces the assembled ladders to curve and eventually become closed rings. Unlike the symmetrical, homodimeric motifs used in the straight nanoladders, asymmetrical, heterodimeric motifs (M3 and M4) were used for nanoring assembly. Each motif consists of a long, hairpin-containing strand (H3 or H4) for HCR and a short strand (T3 or T4) for T-junction cohesion (M3: H3 + T3; M4: H4 + T4). The motif is organized into three domains: a 10 bp central duplex as a spacer, a short arm for T-junction cohesion, and a long hairpin arm for HCR. The two involved motifs possess identical short arms for T-junction cohesion, but two complementary, long arms for alternating HCR assembly. T-junction cohesion can happen at any time and results in a helical domain with a length of 5 bps. Such an intermotif interaction by itself is not stable under the current experimental conditions. In contrast, HCR will not occur until an initiator is added to open up the hairpin structure of the first M3 motif. HCR produces stable interactions and results in linear polymers consisting of alternating motifs M3 and M4. Along the already formed polymer chains, the T-junction cohesion becomes stable because of less entropy loss. The resulting polymer can be viewed as a ladder consisting of two long, parallel duplexes (one from T-junction cohesion and the other from HCR) separated by a series of 10 bp duplex spacers. However, the two long duplexes have different lengths (1 helical turn per motif for the T-junction duplex, and 2.5 helical turns per motif for the HCR duplex), which cause the ladder to bend towards the shorter duplex. Cumulative bending leads the ladder to form a pseudocircular conformation.

We developed a two-step toehold displacement for the purpose of closing the circle (Figure 1 d). The 9 nucleotide (nt) long single-stranded toehold region on the hairpin arm of strand H3 in M3 is divided into two segments: the initiation toehold and the termination toehold. The initiator strand (IR) is designed to be only complementary to the initiation toehold (3–6 nt long), but not the termination toehold. It can bind to M3 and open the hairpin structure of strand H3, thus initiating HCR. When the pseudocircular ladder forms, the last incorporated M4 unit is proximate to the head IR–M3 motif and can replace IR by termination-toehold-mediated strand displacement with its newly released tail, which is fully complementary to the 9 nt long toehold region (including both the initiation toehold and the termination toehold) of M3 (Figure 1 d). Eventually, a fully closed DNA nanoring is assembled, and the initiator (IR) is released from the nanoring (Figure 1 c).

DNA-nanoring assembly was first tested with IR-5. After assembly, the DNA samples were analyzed by electrophoresis (Figure 3 a). The assembled DNA complexes appeared as one distinct band, whose mobility remained constant at different IR-5/M3/M4 ratios. This observation suggested that the DNA complexes were closed structures with finite sizes and a narrow molecular-weight (MW) distribution. The result was dramatically different from that for the assembly of DNA nanoladders (Figure 2 a), in which case DNA complexes with a wide MW distribution appeared as a continuous smear, and their MW increased as the M/IL ratio increased (see Figure S2 a). Direct visualization by AFM imaging further confirmed the formation of DNA nanorings (Figure 3 b,c; see also Figures S3 and S4). On the surfaces, randomly distributed ring structures could easily be seen. Their diameters were (38 ± 6) nm, which corresponds to roughly 12–14 motifs per ring. The nanorings were not uniform in size, but instead had quite a large distribution. Besides the nanorings, there were some undesired, larger aggregates. On the basis of the band intensities in the fourth lane of Figure 3 a, the nanoring yield was estimated to be approximately 50%.

One important factor influencing the nanoring assembly is the length arrangement of the initiation toehold and termination toehold (see Figure S5). To investigate this effect, we designed four versions of the IR strand: IR-3, IR-4, IR-5, and IR-6. The number indicates how many nucleotides long the

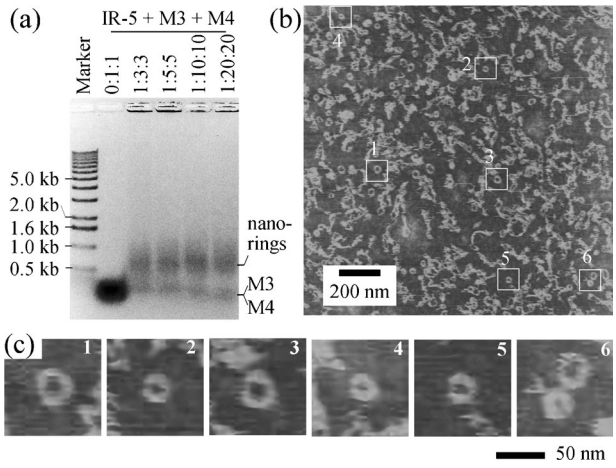

Figure 3. Analysis of the self-assembly of DNA nanorings. a) Native agarose gel (1%) electrophoresis. Sample compositions were indicated above the gel, and the chemical identity of the bands is suggested beside the gel. For electrophoresis, the DNA concentrations were 500 nM M3, 500 nM M4, and a varying concentration of IR-5 according to the indicated molar ratio. b) Large-area AFM image of the DNA assemblies. c) Close-up views of six nanorings in the AFM image, as indicated. For AFM imaging, the DNA concentrations were 100 nM IR-5, 500 nM M3, and 500 nM M4.

initiation toehold is. For example, the initiation toehold of strand IR-3 has a length of 3 nt. Consequently, the termination toehold is 6 nt long, since the sum of the initiation toehold and termination toehold is 9 nt. For IR-3, the short, 3 nt long initiation toehold is too short and can not efficiently initiate the assembly process; however, the corresponding 6 nt long termination toehold is long enough to terminate the assembly. Consequently, a large amount of monomers (M3 and M4) remain, and only a small amount of nanorings form. This phenomenon is evidenced by both gel electrophoresis (see Figure S5a) and AFM imaging (see Figure S5b). As the length of the initiation toehold increases to 5 nt (IR-5), the initiation becomes very efficient. The corresponding 4 nt long termination toehold is also strong enough (for the intracomplex reaction) to terminate the assembly and close the ring (Figure 3). When the initiation toehold length is further increased to 6 nt (IR-6), the initiation becomes very efficient; however, the corresponding termination toehold with a length of 3 nt is too short for assembly termination, thus leading to large aggregates, which can not penetrate into the gel matrix and therefore stay in the well (see Figure S5a).

In summary, we have developed a concept for synchronizing two assembly processes on the basis of proximity and have applied this concept to the assembly of DNA nanoladders and nanorings in response to external stimuli under isothermal conditions. The synchronization was possible by bringing two processes into proximity to promote positive synergy. With further development, synchronization might become a general approach to integrate multiple inputs to assemble complex DNA nanostructures through multiple assembly mechanisms. It would be particular useful for biomedical research, such as assembly-based biosensing[6] or the organization of chemical reactions in living cells.[7]

Received: April 15, 2014
Published online: June 24, 2014

Keywords: DNA · DNA nanotechnology · DNA nanostructures · self-assembly · strand displacement

[1] a) N. C. Seeman, *Annu. Rev. Biochem.* **2010**, *79*, 65–87; b) A. V. Pinheiro, D. R. Han, W. M. Shih, H. Yan, *Nat. Nanotechnol.* **2011**, *6*, 763–772.
[2] a) P. W. K. Rothemund, *Nature* **2006**, *440*, 297–302; b) Y. He, T. Ye, M. Su, C. Zhang, A. E. Ribbe, W. Jiang, C. D. Mao, *Nature* **2008**, *452*, 198–201; c) J. J. Sobczak, T. G. Martin, T. Gerling, H. Dietz, *Science* **2012**, *338*, 1458–1461; d) R. Jungmann, T. Liedl, T. L. Sobey, W. Shih, F. C. Simmel, *J. Am. Chem. Soc.* **2008**, *130*, 10062–10063.
[3] T. D. Pollard, G. G. Borisy, *Cell* **2003**, *112*, 453–465.
[4] a) R. M. Dirks, N. A. Pierce, *Proc. Natl. Acad. Sci. USA* **2004**, *101*, 15275–15278; b) D. Y. Zhang, R. F. Hariadi, H. M. T. Choi, E. Winfree, *Nat. Commun.* **2013**, *4*, 1965; c) J. P. Sadowski, C. R. Calvert, D. Y. Zhang, N. A. Pierce, P. Yin, *ACS Nano* **2014**, *8*, 3251–3259; d) P. Yin, H. M. T. Choi, C. R. Calvert, N. A. Pierce, *Nature* **2008**, *451*, 318–322.
[5] a) S. Hamada, S. Murata, *Angew. Chem.* **2009**, *121*, 6952–6955; *Angew. Chem. Int. Ed.* **2009**, *48*, 6820–6823; b) J. Lee, S. Hamada, R. Amin, S. Kim, A. Kulkarni, T. Kim, Y. Roh, S. Murata, S. H. Park, *Small* **2011**, *8*, 374–377; c) X. Li, C. Zhang, C. H. Hao, C. Tian, G. S. Wang, C. D. Mao, *ACS Nano* **2012**, *6*, 5138–5142.
[6] a) H. M. T. Choi, J. Y. Chang, L. A. Trinh, J. E. Padilla, S. E. Fraser, N. A. Pierce, *Nat. Biotechnol.* **2010**, *28*, 1208–1212; b) J. Huang, Y. R. Wu, Y. Chen, Z. Zhu, X. H. Yang, C. J. Yang, K. M. Wang, W. H. Tan, *Angew. Chem.* **2011**, *123*, 421–424; *Angew. Chem. Int. Ed.* **2011**, *50*, 401–404; c) G. Z. Zhu, S. F. Zhang, E. Q. Song, J. Zheng, R. Hu, W. H. Tan, *Angew. Chem.* **2013**, *125*, 5600–5606; *Angew. Chem. Int. Ed.* **2013**, *52*, 5490–5496; d) F. Wang, J. Elbaz, R. Orbach, N. Magen, I. Willner, *J. Am. Chem. Soc.* **2011**, *133*, 17149–17151.
[7] C. J. Delebecque, A. B. Lindner, P. A. Silver, F. A. Aldaye, *Science* **2011**, *333*, 470–474.

